J Appl Electrochem (2008) 38:101–108
DOI 10.1007/s10800-007-9406-1

ORIGINAL PAPER

Electrocatalytic oxidation of nitrophenols in aqueous solution using modified PbO_2 electrodes

Huiling Liu · Yuan Liu · Cheng Zhang · Rongshu Shen

Received: 21 August 2006 / Revised: 14 August 2007 / Accepted: 22 August 2007 / Published online: 9 September 2007

Abstract Various kinds of modified lead dioxide (PbO_2) electrodes, doped with bismuth oxides and cobalt oxides, were prepared by electrodeposition in acid solution, and were characterized in terms of their morphological (SEM) and structural (XRD) features. Mineralization experiments on o-nitrophenol (ONP) in an electrocatalytic oxidation system showed that the electrocatalytic activity of Ti/Bi–PbO_2 was superior to the traditional dimensionally stable anodes (DSAs) Ti/β-PbO_2 and other modified PbO_2 electrodes. The mineralization, reaction kinetics and nitro-group transformation of nitrophenols (ONP, p-nitrophenol (PNP) and m-nitrophenol (MNP)) on Ti/Bi–PbO_2 electrodes were studied and compared. NPs were degraded completely under the present experimental conditions by applying a 30 mA cm^{-2} current density at pH 4.3 in 0.1 M Na_2SO_4 and 0.01 M NaCl. The degradation of NPs lay in the order: ONP > MNP > PNP. A simple degradation mechanism model is proposed.

Keywords Electro-catalytic oxidation · Nitrophenols · PbO_2 electrode · Electrodeposition

1 Introduction

Industrial effluents containing toxic and recalcitrant organic compounds lead to severe environmental problems. Traditional treatment methods, including biological, physical and chemical treatment are ineffective, and thus a number of alternatives have been researched, such as supercritical water oxidation [1], photochemical [2] and peroxide/UV treatment [3], etc. Electrochemical degradation (ECD) is one of the alternatives for degradation of these compounds, and is suitable for low-volume application and environmental compatibility [4]. In recent years, electrochemical oxidation of aqueous wastes containing non-biodegradable organics such as phenol [5], chlorophenols [6] and aniline [7] has been extensively studied.

To improve the degradation efficiency various types of electrode, including graphite [8], Pt [9], activated carbon [10], carbon fiber [11], PbO_2 [12], SnO_2 [13], and diamond electrodes [14] have been investigated. A general scheme for the electrochemical degradation of organic compounds on metal oxide electrodes (MO_x) has been proposed [15]. H_2O is assumed to be discharged on the anode to form adsorbed hydroxyl radicals:

$$MO_x + H_2O \rightarrow MO_x(\cdot OH) + H^+ + e^- \quad (1)$$

On the oxide surface, in the presence of oxidizable organic compounds (R), the following reaction takes place and the organics are decomposed by the generated hydroxyl radicals:

$$R + MO_x(\cdot OH) \rightarrow CO_2 + zH^+ + MO_x + ze^- \quad (2)$$

Many researchers agree with these "hydroxyl radical oxidation" mechanisms. Based on these mechanisms many specific degradation pathways for different organics have been investigated through intermediate determination [16, 17].

Since Beer [18] developed dimensionally stable anodes (DSAs) these have been studied due to their good stability and catalytic activity. Recently, there has been an interest in the improvement of lead dioxide (PbO_2) as an anode material for electro-synthesis [19], ozone generation [20]

H. Liu (✉) · Y. Liu · C. Zhang · R. Shen
Department of Environmental Science & Engineering, Harbin Institute of Technology, Harbin 150090, China
e-mail: hlliu2002@163.com

and wastewater treatment [21], owing to its high electrical conductivity, high oxygen overpotential and chemical inertness. PbO_2 can be easily obtained by anodic deposition from the solution of low-valence lead ions. However, the electrochemical properties of electrodeposited PbO_2 are strongly affected by doping species present in the deposition bath, especially metal cations [22, 23]. Some researchers [19, 24–27] have chosen Bismuth, Cobalt, Cerium and Iron as dopants to change certain characteristics of the PbO_2 electrode, including catalytic activity and O-atom transfer properties. However, few workers [7] have applied these modified PbO_2 electrodes to the degradation of organics in the environmental field. This stimulated us to think that Bi oxide or Co oxide, as dopants, were in principle, interesting candidates for investigation as anodes.

Nitrophenols (NPs) are manufactured chemicals that cannot be degraded naturally in the environment [28]. NPs are common components of industrial effluents and have been detected in urban and agricultural wastes. NPs are intermediates in the syntheses of pesticides and dyes, and are often found in wastewater as a result of the tropospheric transformation of alkyl benzenes. These compounds pose significant health risks since they are carcinogenic [29]. Indeed, o-nitrophenol and p-nitrophenol are listed on the US Environmental Protection Agency's (USEPA) "Priority Pollutants List". The USEPA recommends restricting their concentration in natural waters to below 10 ng L^{-1} [30, 31], as it takes a long time for NPs to break down in groundwater, as well as in deep soil. The destruction and mineralization of NPs in waste streams are now possible by utilizing advanced oxidation processes (AOPs), such as, Fenton [32], photocatalytic oxidation [33, 34], sonochemical degradation [35] and electrochemical degradation [36–40], but satisfactory methods are still undeveloped and their degradation mechanism is not clear.

The present work describes the modifications made to improve anode electrocatalytic activity, with a view to wastewater treatment using nitrophenolic compounds as model pollutants and studying the degradation rate. In this study, four kinds of modified PbO_2 electrodes were doped with the oxides of Bi and Co. The morphologies and structure of the deposited lead dioxide film were studied by SEM and XRD. Electrocatalytic oxidation of NPs using modified PbO_2 anodes was investigated, and a simple degradation mechanism model is proposed.

2 Materials and methods

2.1 Materials

High-purity (99.5%) titanium plates with a reaction area of 50×10 mm^2 were selected as the metal matrix. A stainless steel sheet with the same area as the titanium sheet was used as a cathode. The main chemical reagents were lead nitrate, sodium sulfate, stadium chloride, tin chloride, antimony chloride, powder blue, bismuth nitrate and n-butanol. All chemical reagents were analytical grade. Solutions were prepared using deionized *Milli-Q* water.

2.2 Analysis

Scanning electronic microscopy (SEM; Japan Hitachi S-570) was used to study the surface morphology of the modified PbO_2 electrodes. The crystalline structure of the modified PbO_2 electrodes was examined using a D/max-rB X-ray diffraction with CuKα radiation ($\lambda = 1.54050$). Measurements were performed at 0.018° intervals of 2θ over the range of 20–100° with a count-time of 10 s per step.

NPs concentration was measured with a LC-10A High Performance Liquid Chromatograph equipped with a flame ionization detector (FID). Aliquots of 10 μL were injected automatically into the HPLC to determine the concentration of NPs, using a mobile phase of methanol/water (v/v) at 70/30. The separation was performed using a Vp-ODS reversed phase column at the flow rate of 1 mL min^{-1} under 28 MPa pressure and column temperature of 303 K. Before the analysis, the mobile phase was filtered and sonicated in order to remove dissolved gas. A UV detector was used with the wavelength set at 280 nm. Nitrogen inorganic ions (NO_3^-, NO_2^-) were measured with an ion chromatograph (DIONEX 4500i) equipped with an electrical conductivity detector (ECD). Aliquots of 25 μL were injected into the IC, and carried with a mobile phase containing 1.7 mM $NaHCO_3$ and 1.8 mM Na_2CO_3. The separation was performed using a HPIC-AG4-AS4A-SC phase column at the flow rate of 1 μL min^{-1} under 780 psi. The TOC of the system was analyzed using a TOC Analyzer (SHIMADZU TOC 5000A).

2.3 Preparation of lead dioxide

The Ti plates were polished with sand paper and then cleaned using ultrasound for 10 min to remove sand particles lodged in the metal. Ti plates were degreased in 40% NaOH solution for 2 h at 313 K. Next, these plates were pretreated by etching in boiling 10% oxalic acid for 2 h until TiO_2 was thoroughly dissolved and a reddish-brown titanium oxalate was produced. Then the Ti plates were conserved in an aqueous solution of 1% oxalic acid to avoid the re-formation of TiO_2.

A liquid mixture consisted of $SnCl_4{\cdot}H_2O$, $SbCl_3$ dissolved in n-butanol-HCl solution was painted on the Ti plates. The solution was then evaporated under infrared light at 373 K and the same paint-evaporation procedure was repeated four times. The Ti plates were then thermally treated in a muffle furnace at 773 K for 2 h to prepare undercoatings of SnO_2 and Sb_2O_5. An interlayer of α-PbO_2 was then electrodeposited above undercoating from alkaline solution. Finally, a surface of β-PbO_2 was electrodeposited on the top of α-PbO_2 interlayer from an acidic solution.

2.4 Electrocatalytic oxidation

The electrocatalytic oxidation experiments were carried out by batch processes and the apparatus was mainly consisted of a potentiostat, a magnetic stirrer, a water bath and a glass reactor. The anode and cathode were positioned vertically and parallel to each other.

NPs with an initial concentration of 50 mg L^{-1} were selected as model organic pollutants and the volume of NPs solution was 300 mL. 0.1 M Na_2SO_4 was used as a supporting electrolyte. 0.01 M NaCl was used as a chlorine ion supplementing solution. The pH and temperature of the ONP solution were 4.3 and 333 K, respectively. Electrocatalytic oxidation was performed under galvanostatic control at a current density of 30 mA cm^{-2}. During the experiments samples were drawn from the reactor at certain intervals and then analyzed.

3 Results and discussion

3.1 Investigation of PbO_2 electrodes

3.1.1 Physical characteristics of PbO_2 electrodes

The doping of different metallic oxides into the surface of β-PbO_2 was evident in the SEM micrographs of the PbO_2 film. The SEM micrographs of the modified PbO_2 electrodes (Ti/Co–PbO_2, Ti/Bi–PbO_2 and Ti/Co–Bi–PbO_2) and traditional PbO_2 electrode (Ti/β-PbO_2) are shown in Fig. 1. Compared with the three other lead dioxide electrodes, Ti/Bi–PbO_2 has a porous structure with small-sized crystal particles and a very compact crystalline structure (Fig. 1b). The characteristics mentioned above favor the enlarged specific surface area of an electrode. Compared with Ti/β-PbO_2, Ti/Co–PbO_2 and Ti/Co–Bi–PbO_2 have smaller particles (Fig. 1c and d).

Figure 2 presents the XRD patterns of PbO_2 electrodes. All the patterns clearly show the characteristic reflections of β-PbO_2 with a tetragonal structure, in accordance with the literature [41]. Using calculations, the crystal sizes and crystal cell parameters were obtained and presented in Tables 1 and 2. The data in Table 1 are consistent with the conclusion of the SEM micrographs, namely that Bi doping can diminish the size of the crystal particles. It can be seen from the comparison of Fig. 2a, b and d that Bi doping could widen the PbO_2 diffraction peaks, weaken their intensities and decrease their corresponding diffraction angles (2θ). This phenomenon demonstrates that PbO_2 crystallites have the tendency to transform to the

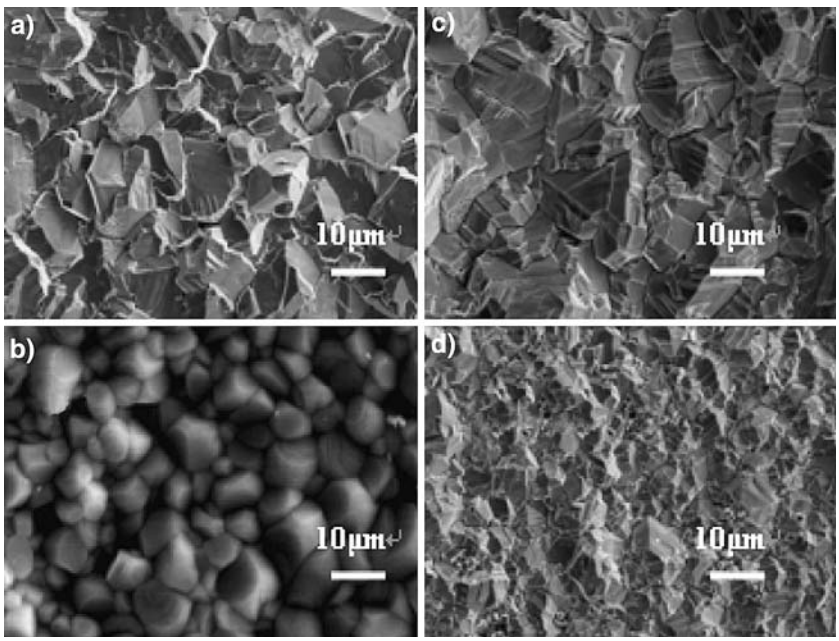

Fig. 1 Scanning electron microscopy micrographs of different PbO_2 electrodes: (**a**) Ti/β-PbO_2; (**b**) Ti/Bi–PbO_2; (**c**) Ti/Co–PbO_2; (**d**) Ti/Co–Bi–PbO_2

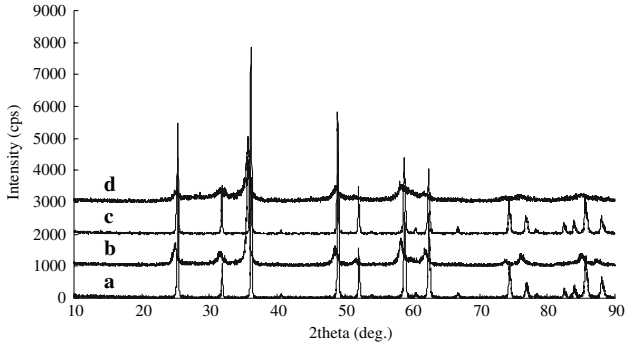

Fig. 2 X-ray Diffraction patterns of different PbO_2 electrodes: (**a**) Ti/β-PbO_2; (**b**) Ti/Bi–PbO_2; (**c**) Ti/Co–PbO_2; (**d**) Ti/Co–Bi–PbO_2

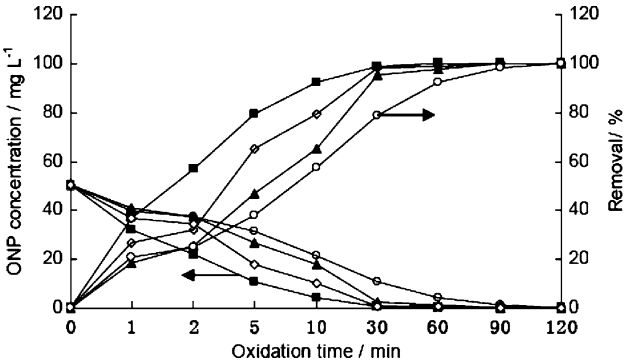

Fig. 3 Variation of ONP concentration with time on different PbO_2 electrodes: (-■- Ti/Bi–PbO_2); (-▲- Ti/Co–PbO_2); (-○- Ti/Co–Bi–PbO_2); (-◇- Ti/β-PbO_2), $[ONP]_0$ = 50 mg L^{-1}; pH = 4.3; temperature = 353 K; current density = 30 mA cm^{-2}; $[Na_2SO_4]$ = 0.1 M; [NaCl] = 0.01M

Table 1 Crystal sizes of different PbO_2 electrodes

	Ti/Bi–PbO_2	Ti/Co–Bi–PbO_2	Ti/β-PbO_2	Ti/Co–PbO_2
Crystal sizes/nm	17.491	19.467	27.929	27.057

amorphous state, which might be attributed to the fact that Bi doping resulted in crystal cell expansion (see Table 2) and structure defects. Moreover, Co doping had no effect on the PbO_2 crystallites, but only slightly decreased the intensities of the diffraction peaks in terms of the comparison between Fig. 2a and c. In Fig. 2, none of the diffraction peaks corresponding to Bi_2O_5 and Co_2O_3 were found. This may be due to their low contents, because the mole ratios of bismuth atoms to lead atoms, and cobalt atoms to lead atoms, were 1:100 and 1:200, respectively.

3.1.2 *Electrocatalytic oxidation of ONP on PbO_2 electrodes*

ONP was totally degraded after 2-h electrocatalytic oxidation, as shown in Fig. 3. In this study, the pseudo-first kinetics of ONP on these four electrodes was obtained. The formula can be described as following:

$$dC_{NP}/dt = -\mathrm{K}_1 C_{NP},$$

where K_1 is the pseudo-first order rate constant. The kinetics coefficients K are listed in Table 3. These experimental results indicate that the incorporation of Bi_2O_5 oxide into the surface of the PbO_2 electrode could enhance the electrocatalytic activity of the electrode.

3.1.3 *TOC removal of ONP on PbO_2 electrodes*

The Ti/Bi–PbO_2 electrode has the highest TOC removal of ONP (87.0%), followed by Ti/Co–Bi–PbO_2, Ti/β-PbO_2 and Ti/Co–PbO_2, whose TOC removals are 83.3%, 77.8% and 75.9%, respectively, as shown in Fig. 4. Compared with Ti/β-PbO_2, the electrocatalytic activity of Ti/Bi–PbO_2 is higher and the TOC removal increases by nearly 10%. Also, the electrocatalytic activity of Ti/Co–PbO_2 decreases, as compared with a pure β-PbO_2 electrode. The incorporation of Co oxide into the PbO_2 electrode may reduce the oxygen evolution overvoltage, which induces oxygen evolution on Ti/Co–PbO_2 much easier than on Ti/β-PbO_2 [42, 43]. Therefore, the oxidation of organic compounds was diminished on Ti/Co–PbO_2, which led to a lower TOC removal. The good electrocatalytic activity of the Ti/Bi–PbO_2 electrode might be associated with the doping manner of Bi atoms in PbO_2. On the one hand, Bi doping diminished the size of the crystal particles, which had a positive influence on increasing the specific surface area and enhancing the activity of the electrode, while on the other hand, Bi doping resulted in crystal cell expansion and structure defects. These two factors increased the

Table 2 Crystal cell parameters of different PbO_2 electrodes

	Ti/Bi–PbO_2	Ti/Co–Bi–PbO_2	Ti/β-PbO_2	Ti/Co–PbO_2
a = b/nm	0.504	0.501	0.496	0.497
c/nm	0.356	0.354	0.351	0.351
$V = a*b*c$/nm^3	0.0904	0.0889	0.0864	0.0867
Expansion coefficient	1.047	1.029	1	1.004

Table 3 Comparison of coefficient *K* values calculated based on the tests

PbO_2 electrodes	K/min^{-1}	Correlation coefficient R^2
Ti/Bi–PbO_2	0.0988	0.9723
Ti/Co–PbO_2	0.0712	0.9745
Ti/Co–Bi–PbO_2	0.0411	0.9885
Ti/β-PbO_2	0.0738	0.9411

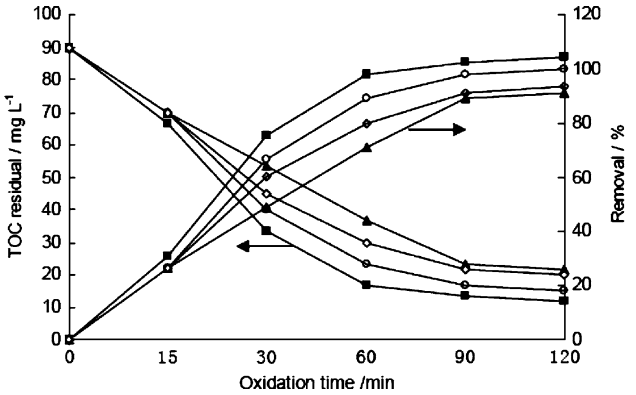

Fig. 4 Variation of TOC amounts of ONP with time on different PbO_2 electrodes: (-■-) Ti/Bi–PbO_2; (-▲-) Ti/Co–PbO_2; (-○-) Ti/Co–Bi–PbO_2; (-□-) Ti/β-PbO_2, $[ONP]_0$ = 50 mg L^{-1}; pH = 4.3; temperature = 353 K; current density = 30 mA cm^2; $[Na_2SO_4]$ = 0.1 M; [NaCl] = 0.01 M

active sites on the surface of the PbO_2 electrode, making it more conducive to the generation of hydroxyl radicals so as to enhance the electrocatalytic activity of this electrode, a result which coincided with the conclusion of reference [25].

3.1.4 Current efficiency (CE)

The current efficiency of each PbO_2 electrode is expressed in the following equation,

$$\xi = \frac{\Delta TOC \cdot F \cdot V}{8I \cdot \Delta t \cdot 1,000} \times 100\%,$$

where ΔTOC is the amount of *TOC* removal (mg L^{-1}), F is the Faraday constant (96487 C mol^{-1}), V is the volume of electrolyte solution (L), Δt is the degradation time (s), and I is the current intensity (A).

At the end of the reaction, Ti/Bi–PbO_2 has the highest current efficiency, followed by Ti/β-PbO_2, Ti/Co–PbO_2 and Ti/Co–Bi–PbO_2, whose CE are 75.6%, 74.0%, 67.6% and 65.9%, respectively, as shown in Table 4. The result indicates that the Bi–PbO_2 modified electrode lowers the energy-consumption of electrocatalytic oxidation.

Table 4 Current efficiency of ONP on different PbO_2 electrodes

	Ti/Bi–PbO_2	Ti/Co–Bi–PbO_2	Ti/β-PbO_2	Ti/Co–PbO_2
CE/ξ%	75.6	74.0	67.6	65.9

3.2 Electrocatalytic oxidation of NPs on Ti/Bi–PbO_2 electrode

According to the results presented above it is known that Ti/Bi–PbO_2 has higher electrocatalytic activity. To investigate the degradation of NPs, the Ti/Bi–PbO_2 electrode was chosen as the working anode.

3.2.1 TOC removal of NPs

Compared to ONP, the TOC removal of MNP and PNP are 82.8% and 81.5%, respectively, as presented in Fig. 5. During the first 1 h, the TOC removal of ONP is about 80%, while the values corresponding to PNP and MNP are 66.7% and 69.0%, respectively. This indicates that ONP may be electrocatalytically oxidized more easily than PNP and MNP. From this figure, it can also be anticipated that TOC removal would be further improved with extended electrocatalytic oxidation.

3.2.2 Degradation kinetics of NPs

The decrease of NP concentration with time is shown in Fig. 6. The complete degradation of the NPs was achieved within 2 h. Electrocatalytic oxidation for the degradation of NPs is satisfactory. During the first 1 h, the ONP degradation was over 99%. It can also be seen from this figure that of ONP, MNP and PNP, ONP degraded fastest, while the degradation rate of MNP was higher than that of PNP.

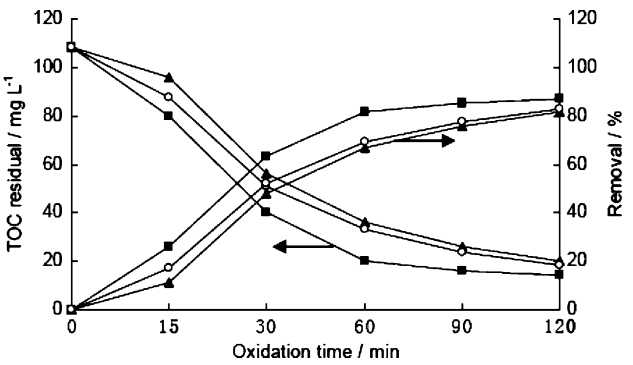

Fig. 5 Variation of TOC amounts of NPs with time on Ti/Bi–PbO_2: (-■-) ONP; (-○-) MNP; (-▲-) PNP, $[NP]_0$ = 50 mg L^{-1}; pH = 4.3; temperature = 353 K; current density = 30 mA cm^2; $[Na_2SO_4]$ = 0.1 M; [NaCl] = 0.01 M

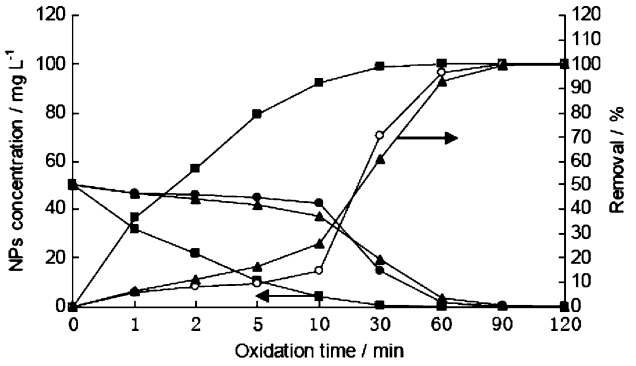

Fig. 6 Variation of NPs concentration with time on Ti/Bi–PbO_2: (-■-) ONP; (-○-) MNP; (-▲-) PNP, $[NP]_0$ = 50 mg L^{-1}; pH = 4.3; temperature = 353 K; current density = 30 mA cm^2; $[Na_2SO_4]$ = 0.1 M; [NaCl] = 0.01 M

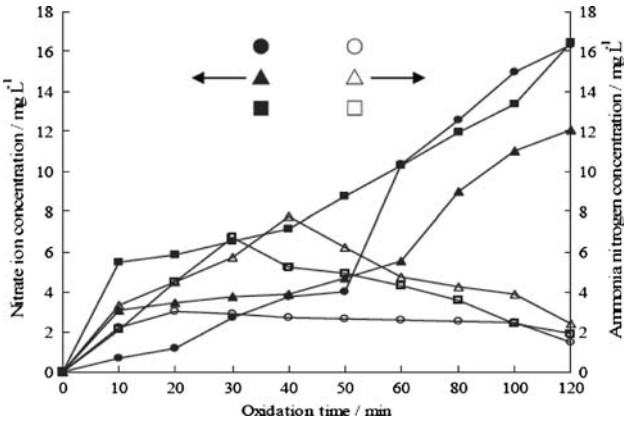

Fig. 7 Nitro-group transformation of NPs on Ti/Bi–PbO_2: (-■, □-) ONP; (-●, ○-) MNP; (-▲,□-) PNP

This indicates that electrochemical oxidation is an effective method for the decomposition of NPs.

Previous study suggested that the degradation of some NPs follows pseudo-first order kinetics [19, 32]. The regression analysis of the concentration curves versus reaction time indicated that the decomposition rate of NPs could also be described by the pseudo-first order kinetics formula with respect to NP concentration: $dC_{NP}/dt = -kC_{NP}$. The kinetic coefficients K listed in Table 5 suggest that the degradation of NPs lies in the order: ONP > MNP > PNP.

3.2.3 *Nitro-group transformation and mechanism of degradation*

The transformation regularity of the nitro-groups of NPs was evaluated in this study and the results are presented in Fig. 7. The results suggest that the nitro-group detached from the aromatic ring was mainly in the form of nitrate and ammonia. However, generally speaking, the nitro-groups were mainly transformed to nitrate radicals. Nitrite ions were not found in the reaction systems, which might be related to the low concentration of nitrite ions due to their short lifetime in solution. The initial concentration of organic nitrogen in the NP reaction system was 0.36 mM, and the total inorganic nitrogen concentrations of ONP, MNP and PNP were 0.353, 0.346 and 0.327 mM, respectively, at the end of reaction. The mass balance results for nitrogen revealed that the nitro-groups of both ONP and MNP were almost completely removed from the aromatic ring.

Table 5 Comparison of coefficient K values calculated based on the tests

Nitrophenols	K/min^{-1}	Correlation coefficient R^2
ONP	0.0988	0.9723
PNP	0.0513	0.9157
MNP	0.0709	0.9750

The mechanism of electrocatalytic oxidation using a PbO_2 electrode includes direct and indirect oxidation. In the direct process, direct oxidation takes place at the electrode surface. Simultaneously, hydroxyl radicals electrogenerated by the water discharge in the regions very close to the electrode remove the organics. In the indirect process, active chlorine can degrade organics in the bulk solution. According to previous studies [38, 44, 45] and our experimental results, a simple degradation mechanism model is proposed as follows: firstly, an additive reaction occurs at the para position of NPs. However, the reactions of PNP and MNP are more difficult than that of ONP due to the influence of the nitro-groups. These nitro-groups are attacked by hydroxyl radicals causing them to become detached from the aromatic rings. Then, some fractions of the released nitro-groups are oxidized to nitrate ions at the anode. The other fraction diffuses to the cathode where they are reduced to ammonia. As demonstrated in Fig. 7, the variation of ammonia concentration with time suggests that the ammonia is re-oxidized in the reaction system. In the initial period of the present experiment, the electrolyte color of ONP and PNP turned to light yellow. Then, the color became darker after a period of time and finally became colorless again. This phenomenon suggests that quinonic compounds were produced during electrocatalytic oxidation. Then, the quinonic compounds are degraded to various carboxylic acids. As for MNP, the color of the electrolyte faded gradually and finally also became colorless; i.e. quinonic compounds did not appear. Finally, these carboxylic acids were all oxidized to CO_2 and H_2O. The degradation pathways of NPs are illustrated in Fig. 8.

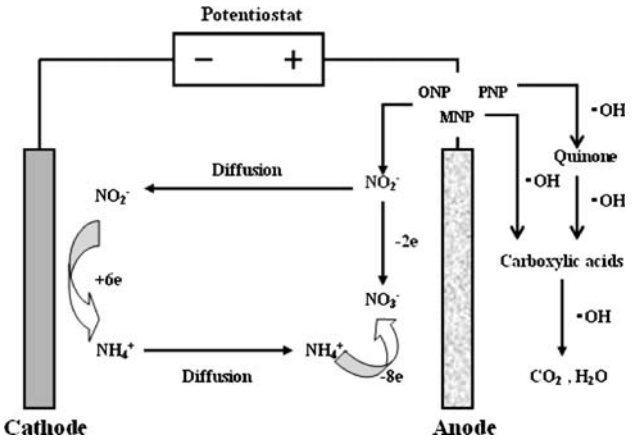

Fig. 8 Sketch of degradation mechanism model of NPs on Ti/Bi–PbO_2

4 Conclusion

Bi doping diminishes the size of PbO_2 crystal particles resulting in crystal cell expansion, which enhances the electrocatalytic activity of the PbO_2 electrode. TOC removal is increased by 10% of ONP on a Ti/Bi–PbO_2 electrode compared with that on Ti/β-PbO_2. The current efficiency on Ti/Bi–PbO_2 is the highest of all PbO_2 electrodes.

The decomposition rate of NPs can be described by pseudo-first order kinetics. The degradation of NPs lies in the order: ONP > MNP > PNP. The nitro-group detaches from the aromatic ring, and is mainly in the forms of nitrate and ammonia. In addition, the nitro-group is mainly transformed into nitrate radicals. As for the degradation of organic compounds, on the one hand, ONP and PNP are firstly oxidized to quinonic compounds and then further oxidized to various carboxylic acids. On the other hand, MNP is firstly oxidized to form carboxylic acids, which are eventually oxidized to CO_2 and H_2O.

Acknowledgements The authors thank the Scientific Research Foundation of Harbin Institute of Technology (No. HIT. 2001.56) for financial support of this work. This research is also supported by Program for Changjiang Scholars and Innovative Research Team in University (PCSIRT), the Ministry of Education.

References

1. Blaney CA, Li L, Gloyna EF, Hossain SU (1995) In: ACS Symposium Series 608. American Chemical Society, Washington, DC, 444 pp
2. Vohra MS, Tanaka K (2002) Water Res 36(1):59
3. Steensen M (1993) Proceedings of the Sardinia 93, Fourth International Landfill Symposium, vol. I, CISA publisher, Cagliari, 945 pp
4. Walsh F, Mills G. (1993) Chem Ind 8(15):576
5. Canizares P, Diaz M, Dominguez JA (2002) Ind Eng Chem Res 41(17):187
6. Zanta CLPS, Michaud PA, Comninellis Ch, De Andrade AR, Boodts JFC (2003) J Appl Electrochem 33(12):1211
7. Brillas E, Bastida RM, Liosa E, Casado J (1995) J Electrochem Soc 142(6):1733
8. Awad YM, Abuzaid N (1999) Sep Sci Technol 34(4):699
9. Comninellis Ch, Pulgarin C (1991) J Appl Electrochem 21(8):703
10. Canizares P, Dominguez JA, Rodrigo MA, Villasenor J, Bodriguez J (1999) Ind Eng Chem Res 38(10):3779
11. Kuramitz H, Nakata Y, Kawasaki M, Tanaka S (2001) Chemosphere 45(1):37
12. Kirk DW, Sharifian H, Foulkes FR (1985) J Appl Electrochem 15(2):285
13. Pulgarin C, Adler N, Peringerv P, Comninellis Ch (1994) Water Res 28(4):887
14. Chen XM, Chen GH, Gao FR, Yue PL (2003) Environ Sci Technol 37(21):5021
15. Canizares P, Martinez F, Diaz M, Garcia-Gomez J, Rodrigo MA (2002) J Electrochem Soc 149(8):D118
16. Johnson SK, Houk LL, Feng J, Houk RS, Johnson DC (1999) Environ Sci Technol 33(15):2638
17. Oturan MA, Peiroten J, Chartrin P, Acher AJ (2000) Environ Sci Technol 34(16):3474
18. Beer HB (1976) US Patent 3632498
19. Ai SY, Gao MN, Zhang W, Wang QJ (2004) Talanta 62(3):445
20. Amadelli R, Armelao L, Velichenko AB, Nikolenko NV, Girenko DV, Kovalyov SV, Danilov FI (1999) Electrochimica Acta 45(4–5):713
21. Johnson DC, Feng J, Houk LL (2000) Electrochimica Acta 46(2–3):323
22. Pamplin KL, Johnson DC (1996) J Electrochem Soc 143(7):2119
23. Velichenko AB, Amadelli R, Zucchini GL, Girenko DV, Danilov FI (2000) Electrochimica Acta 45(25–26):4341
24. Fu WT, Martens HCF (2000) Solid State Commun 115(8):423
25. Popovic ND, Cox JA, Johnson DC (1998) J Electrochem Chem 455(1–2):153
26. Cattarin S, Frateur I, Guerriero P, Musiani M (2000) Electrochimica Acta 45(14):2279
27. Tahar NB, Savall A (1999) J Appl Electrochem 29(3):277
28. ATSDR (Agency for Toxic Substance, Disease Registry) (1992) Toxicological Profile for NPs. Department of Health and Human Service, Public Health Service, Atlanta, GA, US
29. Podeh MRH, Bhattacharya SK (1996) Water Sci Technol 34(5–6):345
30. Podeh MRH, Bhattacharya SK, Qu MB (1995) Water Res 29(2):391
31. Keith L, Telliard W (1979) Environ Sci Technol 13(4):416
32. Goi A , Trapido M (2002) Chemosphere 46(6):913
33. Egerton TA, Christensen PA, Harrison RW, Wang JW (2005) J Appl Electrochem 35(7–8):799
34. Priya MH, Madras G (2006) Ind Eng Chem Res 45(2):482
35. Sivakumar M, Tatake PA, Pandit AB (2002) Chem Eng 85(2–3):327
36. Baeza A, Ortiz JL, Gonzalez I (1997) J Electroanal Chem 429(1–2):121
37. Borras C, Laredo T, Scharifker BR (2003) Electrochimica Acta 48(19):2775
38. Canizares P, Saez C, Lobato J, Rodrigo MA (2004) Ind Eng Chem Res 43(9):1944
39. Quiroz MA, Reyna S, Martínez-Huitle CA, Ferro S, De Battisti A (2005) Appl Catal: B-Environ 59(3–4):259
40. Wu ZC, Cong YQ, Zhou MH, Tan TE (2005) Chem Eng 106(1):83
41. Powder diffraction file JCPDS 35:1422

42. Musiani M, Furlanetto F, Guerriero P (1997) J Electroanal Chem 440(1–2):131
43. Cattarin S, Guerriero P, Musiani M (2001) Electrochimica Acta 46(26–27):4229
44. Feng YJ, Li XY (2003) Water Res 37(10):2399
45. Zhou MH, Dai QZ, Lei LC, Ma CA, Wang DH (2005) Environ Sci Technol 39(1):363